Stem Cell Research & Therapy

RESEARCH

Open Access

Therapeutic potential of placenta-derived stem cells cultivated on noggin-loaded nanochitosan/polypyrrole-alginate conductive scaffold to restore spinal cord injury

Asma Manzari-Tavakoli[1†], Amirhesam Babajani[1†], Nasim Vousooghi[2], Ali Moghimi[3], Roghayeh Tarasi[1], Fahimeh Safaeinejad[6], Samira Norouzi[4], Soheyl Bahrami[5] and Hassan Niknejad[1*]

Abstract

Objective Spinal cord injury (SCI) is a severe and permanent nerve damage condition that poses significant burdens on individuals and society. Various therapeutic approaches have been explored to mitigate the consequences of SCI. Tissue engineering and regenerative medicine have emerged as a promising avenue for addressing this issue. This study aims to investigate the potential of a nanochitosan/polypyrrole-alginate conductive scaffold, loaded with the Noggin growth factor, an inhibitor of BMP-4 signaling, and human amniotic epithelial cells (hAECs), in promoting the regeneration of SCI in animal models.

Methods The attachment and distribution of isolated hAECs on a fabricated nanochitosan/polypyrrole-alginate conductive scaffold were assessed using SEM. Additionally, the neural differentiation of hAECs on the scaffold was investigated by analyzing the expression of specific neuronal (Calca, Fox3), oligodendrocyte (MBP), and astrocyte (GFAP) genes in vitro. To evaluate the combined effect of the scaffold and Noggin growth factor in animal models, a Noggin-loaded scaffold was designed using bioinformatics, and the loading and release capacity of Noggin were measured. For in vivo studies, rats underwent laminectomy and were transplanted with the scaffold, either alone or with Noggin and DII labeled- hAECs, at the T10-T11 level. Motor functions of the animal were evaluated using BBB scoring weekly in an open field for four weeks. Furthermore, the expression of neural genes and immunohistochemical tests were evaluated after four weeks.

Results hAECs exhibited uniform distribution and attachment to the scaffold. In vitro differentiation analyses showed increased expression of Calca, Fox3, MBP, and GFAP genes. Docking results indicated that Noggin could

†Asma Manzari-Tavakoli and Amirhesam Babajani share the first authorship.

*Correspondence:
Hassan Niknejad
niknejadh@yahoo.com; niknejad@sbmu.ac.ir

Full list of author information is available at the end of the article

interact with chitosan nanoparticles through hydrogen bonds. The chitosan nanoparticles effectively loaded 22.6% of exposed Noggin, and the scaffold released 28.5% of the total incorporated Noggin. In vivo studies demonstrated that transplanting nanochitosan/polypyrrole-alginate conductive scaffolds with DiI labeled-hAECs, with or without Noggin, improved motor functions in animal models. The assessment of gene expression patterns in transplanted hAECs revealed that neuronal (Calca, Fox3) and oligodendrocyte (MBP) genes in the injured spinal cord of the animal models were upregulated. Histopathological analysis showed a reduction in inflammation and glial scar formation, while neural fiber regeneration increased in the treated animals. Also, DiI labeled-hAECs in the lesion site were alive after a period of four weeks.

Conclusion Based on these findings, it can be inferred that the integrative therapeutic effects of human amniotic epithelial cells, nanochitosan/polypyrrole-Alginate conductive scaffold, and Noggin (as BMP-4 signaling inhibitor) represents a promising and innovative approach in the field of translational medicine.

Keywords Stem cells, Noggin, Scaffold, Spinal cord injury, Nervous system, Placenta, Amniotic membrane

Introduction

Spinal cord injury (SCI) is devastating central nervous system (CNS) damage that may stem from trauma, spinal bone fracture, and spinal cord ischemic damage [1, 2]. Studies showed an incidence rate of 10.4–83 cases/million/year for SCI globally, which imposes an impressive burden and cost to individuals and societies [3]. During SCI, the direct damage to the spinal cord impairs signal transmission from brain to body, which may result in a broad range of symptoms, including complete (or incomplete) loss of sensation, movement, reflexes, sphincter function, and potential paralysis [4].

Various therapeutic approaches, such as spine immobilization, spinal decompression through surgery, administrating corticosteroids, and rehabilitation, have been applied [5–7]. However, the therapeutic outcomes were disappointing mainly due to neurons' extrinsic and intrinsic repairment inabilities. The extrinsic inhibitory factors, including Nogo, inhibitory chondroitin sulfate proteoglycans, myelin-associated glycoprotein, netrin, and ephrin, are associated with glial scars, myelin debris, and axonal growth inhibition [8]. Besides, exclusive patterns of intracellular pathways of damaged CNS neurons impede the regeneration and reconstruction of functional connections between neuron and their original targets [9]. Thus, considering new therapeutic approaches for SCI and neurodegenerative diseases is necessary.

One of the promising approaches for CNS regeneration is utilizing cell-based therapy (CBT) in order to enhance CNS reconstruction via modulating intra- and extracellular conditions. Various cell sources are being used for CBT with their exclusive pros and cons. Human amniotic epithelial cells (hAECs), isolated from human placentae, possess desirable features that bring them up as a highlighted and attractive source for CBT. The immune-privileged features of hAECs reduce the chance of immune rejection after the transplantation of hAECs. It has been shown that hAECs express immunosuppressive human leukocyte antigens (HLA)-G, while expressing low amounts of immune-stimulating HLAs such as HLA-A, HLA-B, HLA-C, and HLA-DR. These cells can be expanded up to 10 million after six passages without ethical consideration. Besides, hAECs possess low tumorigenicity, display immunomodulatory effects, and secrete several growth factors necessary for tissue regeneration, including epithelial growth factor (EGF), keratinocyte growth factor (KGF), and transforming growth factor (TGF) β [10, 11]. Studies have reported that hAECs express pluripotency transcription factors and stem cell markers, including octamer-binding-protein-4 (OCT-4), tumor rejection antigens (TRA) 1–60, TRA-1-81, fibroblast growth factor (FGF)-4, sex-determining region Y-box 2 (SOX-2), teratocarcinoma-derived growth factor 1 (TDGF1), stage-specific embryonic antigen (SSEA)-3, and SSEA-4, and homeobox protein NANOG [12, 13]. Considering the maintained pluripotency of hAECs, studies have reported that these cells are able to differentiate into endodermal, mesodermal, and ectodermal linage [14]. In this regard, the differentiation potency of hAECs to functional neural cells that synthesize and release neurotransmitters such as acetylcholine, norepinephrine, and dopamine was reported [15, 16]. In order to persuade hAECs to differentiate to ectodermal lineage, modulating evolutionary signaling pathways is critical. Among several pathways involved in the ectodermal differentiation of hAECs, bone morphogenetic protein (BMP) signaling as a constituent molecule in ectodermal fate affecting both neural and keratinocyte differentiation [17]. Recently, we have shown that BMP-4 inhibition by Noggin plays a critical role in the differentiation of hAECs into neural cells [18]. Thus, modulating BMP signaling will persuade hAECs toward a neural fate that provides an appropriate intracellular condition for SCI treatment.

Along with reprogramming stem cells to regenerate functional neurons, it seems that redirecting axonal growth across damaged sites and providing appropriate extrinsic conditions is critical for promoting SCI repair.

In this regard, tissue engineering (TE) approaches have provided scaffolds that maintain desirable cell adhesion, differentiation, and proliferation conditions to regenerate target tissue with proper functions. Various biomaterials from natural or synthetic sources have been studied as a proposed microenvironment for CNS regeneration [19, 20]. Considering the electrical activities within the nervous system, conductive polymers are potential candidates for SCI repair. Recently, we have shown that the nanochitosan/polypyrrole (PPy)–alginate (Alg) scaffold composite displayed high conductivity and potency for neural cell attachment [21]. In the present study, the differentiation of hAECs to neural cells (neuron, oligodendrocyte, and astrocyte) was investigated on the conductive scaffold by Real-Time PCR technique in vitro and in vivo. Also, in order to investigate the synergic effects of scaffold and Noggin (a BMP-4 inhibitor) on repairing damaged spinal cord in vivo, the interaction of nanochitosan particles, as scaffold components with the active site of Noggin protein was investigated using molecular simulation (Bioinformatics). Subsequently, we prepared the scaffold loaded with Noggin, then the efficacy of Noggin loading and release from the designed scaffold was evaluated. For the animal study, a unilateral injury (hemisection) was made at the T10-T11 level of the spinal cord in rats, and nanochitosan/PPy–Alg scaffold alone or together with DII-labeled hAECs, Noggin-loaded scaffold alone or jointly with hAECs labeled with DII, and DII-labeled cells alone were transplanted into the lesion site. After four weeks, motor functions, histology results, and immunohistochemistry tests were evaluated. We hypothesize that the combination of a conductive nanochitosan/PPy–Alg scaffold loaded with Noggin growth factor and hAECs will promote spinal cord regeneration after SCI by enhancing cell attachment, differentiation, axonal redirection, and survival, while simultaneously reducing inflammation and glial scarring.

Materials and methods

Collection of human placentae

All experimental procedures were carried out after approval by the ethics committee of Shahid Beheshti University of Medical Sciences (IR.SBMU.MSP.REC.1401.001). Besides, all methods were performed under the relevant guidelines and regulations. The term human placenta ($n=36$) was provided after elective Cesarean sections. All placentas were obtained from mothers who were negative for viral and bacterial infections such as hepatitis C, hepatitis B, HIV, and syphilis. The human placentae were carried to the laboratory under appropriate sterility and temperature of 4–8 °C. Prior to the collection process, written consent was obtained from each donor.

Isolation and culture of hAECs from human placenta

Human amniotic epithelial cells were isolated according to our previous studies [18, 22, 23]. The mechanically separated amniotic layer was cleaned with cold phosphate-buffered saline (PBS) to eliminate clots and debris. The amniotic membrane (AM) was divided into smaller pieces and digested with trypsin-EDTA enzyme 0.15% (Merck, Germany) at 37 °C for ten minutes. After the second and third 40 min of incubation with trypsin-EDTA enzyme 0.15%, supernatants were collected, and trypsin was neutralized with FBS (Gibco, UK). The supernatants containing hAECs were centrifuged at 1200 rpm for 12 min. Then, hAECs were cultured in Dulbecco Modified Eagle's Medium (DMED) (Gibco, UK) containing 100 U/ml penicillin/streptomycin (Thermo Fisher, USA) and 10% FBS (Sigma-Aldrich).

In vitro studies

Fabrication of nanochitosan/PPy–Alg scaffold

The nanochitosan/PPy–Alg scaffold was fabricated according to our previous study [21]. The process consists of (a) the preparation of polypyrrole–alginate composites, (b) the synthesis of nanochitosan, and (c) the fabrication of nanochitosan/ PPy–Alg scaffold.

Attachment and distribution of hAECs on nanochitosan/PPy–Alg scaffold

The scaffolds were sterilized with 70% ethanol and then washed several times with sterile PBS containing penicillin/streptomycin. Sterilized scaffolds were incubated for 24 h in a complete culture medium to increase the adhesion of cells to the scaffold. The next day, the culture medium was replaced, and 20,000 hAECs were cultured per well on each scaffold in an incubator for 2 h. Then 150 µl of complete culture medium was added to each well and incubated at 37 °C with 5% CO_2 and 95% humidity for one week. The attached cells on the scaffolds were fixed with 2.5% glutaraldehyde for 2 h and dehydrated with different ethanol concentrations (50, 70, 90, and 100%). Finally, the morphology and distribution of hAECs were evaluated on the nanochitosan/PPy–Alg scaffold using a scanning electron microscope (SEM).

Neural differentiation of hAECs cultured on the nanochitosan/PPy–Alg scaffold in vitro

The scaffolds were sterilized with 70% ethanol and then washed several times with sterile PBS containing penicillin/streptomycin. Subsequently, sterilized scaffolds were transferred to a 12-well plate with 2 ml of complete culture medium, and incubated for 24 h at the standard condition described. On the subsequent day, the culture medium was aspirated from each well, and 20,000 hAECs were seeded onto each scaffold and incubated for 2 h under standard conditions to allow cell attachment to the

scaffold. After 2 h, the culture medium was slowly added to each well. The neural differentiation of cells was evaluated after 21 days in four groups: (a) hAECs without scaffolds, (b) hAECs without scaffolds exposed to 50 ng/ml of Noggin growth factor, (c) hAECs cultured on scaffolds without Noggin, and (d) hAECs with scaffolds exposed to 50 ng/ml of Noggin growth factor. For the first seven days period, differentiation culture medium consisting of DMEM supplemented with 10% FBS, 100 IU/mL penicillin-streptomycin, 5 ng/mL of epidermal growth factor (EGF) (Sigma-Aldrich, USA), 1 mM sodium pyruvate (Sigma-Aldrich, USA), 1% insulin/transferrin/selenium (ITS) (Gibco, UK), 2 mM ascorbic acid (Sigma-Aldrich, USA), 10 ng/mL basic fibroblast growth factor (bFGF) (Sigma-Aldrich, USA), and 1 µM retinoic acid (RA) (Sigma-Aldrich, USA) was added to the culture environment according to the previous studies [18]. After seven days, the experimental groups with Noggin (groups b and d) were exposed to Noggin growth factor at a concentration of 50 ng/mL (n=5). To the groups without Noggin (groups a and c), only the differentiation culture medium was added to each well. After the fourteen-day period following the addition of the growth factors, the expression levels of neural markers derived from hAECs (including FOX3, GFAP, Calca, and MBP genes) were analyzed using the real-time PCR technique.

The expression level of neural markers in differentiated hAECs in vitro

After the differentiation period, the expression level of neural markers FOX3, GFAP, Calca, and MBP was evaluated in hAECs using real-time PCR. The RNA was extracted based on the manufacturer's instructions (Biofact, Korea). Accordingly, cDNA was synthesized using the Biofact Kit and stored at -70 °C. Syber green PCR master mix, ABI STEP ONE plus system (Applied Biosystems, USA), and specific gene primers (Table 1), designed by Primer Express software, were used to perform the Real-Time PCR. The expression level of β-actin, a housekeeping gene, was used to normalize FOX3, GFAP, Calca, and MBP genes. The relative expression level was calculated according to the $2^{-\Delta\Delta CT}$ (Livak) analysis method.

Table 1 The sequence of primers used in the study

Gene	Sequence
Fox3	F = 5′TGAGATTTATGGAGGCTA3′ R = 5′CGATGGTGTGATGGTA3′
CalCa	F = 5′GCGGTAATCTGAGTA3′ R = 5′TAGTTGGCATTCTGG3′
GFAP	F = 5′GAAGCAGATGAAGCCA3′ R = 5′GAACCTCCTCCTCGTG3′
MBP	F = 5′ACCTACTGACCCACCTT3′ R = 5′CACGCTGACTACTCCTC3′
β-actin	F = 5′ GCC CTG AGG CAC TCT TCC A3′ R = 5′CGG ATG TCC ACG TCA CAC TTC 3′

The properties of the designed primers are shown in Table 1.

Molecular simulation of Noggin-chitosan interaction

In advance, we performed a molecular simulation study of Noggin, a BMP-4 inhibitor, with chitosan using Maestro 10.2 platform software (Schrödinger, LLC) in order to evaluate the interaction of nanochitosan particles as a scaffold component with active sites of Noggin.

Loading of Noggin on chitosan nanoparticles

After the bioinformatic study, the loading process started by assessing the absorbance of Noggin's concentration range from 0.1 to 0.6 (ng/ml) in PBS at 260 nm wavelength and obtaining the standard curve. The mixture of 0.01 mg of nanochitosan with 5 ml of deionized water and ethanol with a ratio of 1:1 was homogenized by ultrasonication for 15 min. Afterward, 60 µL of Noggin (50 ng/ml) was added to the medium. The reaction mixture was stirred on a shaker for 48 h at ambient temperature and then centrifuged at 5000 rpm for 30 min. The supernatant was collected to assess the absorbance. Finally, the absorbance of the supernatant (unloaded Noggin amount) was evaluated by the UV detector at 260 nm. The loaded Noggin amount and encapsulation capacity were calculated using formulae 1 and 2.

$$EE\% = \frac{Wt - Wf}{Wt} \times 100 \quad (1)$$

$$LC\% = \frac{Wt - Wf}{Wn} \times 100 \quad (2)$$

EE: entrapment efficiency; LC: loading capacity; Wn: the amount of nanochitosan; Wt: the amount of primary Noggin; Wf: the amount of unloaded Noggin.

Fabrication of Noggin-loaded nanochitosan/PPy–Alg scaffold

In order to evaluate the synergism effects of the nanochitosan/PPy–Alg scaffold and Noggin in vivo, the Noggin-loaded nanochitosan with a concentration of 3% was stirred in 1% acetic acid for 30 min. Then PPy–Alg powder (2:10) with a concentration of 1% was added to this mixture, stirred again for 5 h, placed in a freezer at -80 °C for 24 h, and freeze-dried for 48 h.

Investigating the Noggin release from the nanochitosan/PPy-Alg scaffold loaded with Noggin

A release test was performed to investigate the rate and pattern of Noggin release from the Noggin-loaded nanochitosan/PPy–Alg scaffold. This way, the rate of Noggin release from the scaffold was analyzed for 12 days with a spectrophotometer at 260 nm. The scaffolds were

placed in 1 ml of PBS and incubated at 37 °C. At certain intervals, 100 µl of PBS was taken as a sample, and its absorption was measured. Then 100 µl of fresh PBS was replaced. Finally, the amount of released Noggin in different time intervals were calculated based on the obtained standard curve.

In vivo studies

Culture of DII labeled hAECs on nanochitosan/PPy–Alg scaffold and Noggin-loaded nanochitosan/PPy–Alg scaffold

In order to track hAECs in animal studies, we used 1,1′-dioctadecyl-3,3,3′,3′-tetramethylindocarbocyanine perchlorate (DII). The sterilized scaffolds were incubated in a complete DMEM culture medium to enhance cell adhesion to the scaffold. Subsequently, the culture medium was replaced, and 20,000 hAECs labeled with DII dye were seeded onto the scaffold and incubated in the cell incubator for 2 h, allowing the cells to adhere to the scaffold fully. Afterward, the complete culture medium was slowly added, and cells were incubated at 37 °C containing 5% CO2 and 95% humidity. The labeled cells were observed with a fluorescent microscope and then used for transplanting modeled spinal cord lesions.

Animal model preparation

Each of the animal experiments and procedures in this study was approved according to international guidelines and codes approved by the ethics committee of the Ministry of Health. Adult male Wistar rats ($n=36$) with a body weight ranging from 230 g to 260 g were obtained from the animal center of Shahid Beheshti University of Medical Sciences. The animals were kept at constant temperature and humidity (25 °C, 50% ± 5 humidity) under a 12-hour dark/lighting cycle. Besides, they had free access to food and water. On the day of surgery, animals were anesthetized by intraperitoneal (IP) injection of ketamine (60 mg/kg)-xylazine (10 mg/kg) solution under sterile conditions. The study has been conducted and reported in accordance with the ARRIVE 2.0 guidelines.

Establishment of right hemisection SCI model and grafting of the scaffold at the site of the injury

Following the administration of anesthesia, the animal's fur was shaved, and a longitudinal incision was made along the back to expose the vertebral column. Retractors were used to displace the muscle layers on both sides of the vertebral column. Rats were subjected to laminectomy at the level of T10-T11 under aseptic conditions. Following laminectomy, a 2×4 mm cavity was made on the right side of the T10-T11 segment. Rats were randomly divided into six experimental groups for four weeks to evaluate behavioral and histological analyses. (a) SCI group (control) ($n=6$), (b) SCI group transplanted with conductive scaffold without hAECs and Noggin growth factor ($n=6$), (c) SCI group grafted with scaffold cultured with labeled hAECs ($n=6$), (d) SCI group grafted with Noggin-loaded scaffold without hAECs ($n=6$), (e) SCI group grafted with Noggin-loaded scaffold cultured with labeled hAECs ($n=6$) (f) SCI group transplanted with an injection of labeled hAECs alone. In the control group, the injury cavity was empty without any intervention (a). In the treatment groups, scaffolds or scaffolds cultured with hAECs were transplanted into the lesion cavity with the longitudinal axis parallel to the spinal cord, and a piece of fascia was used to fix the scaffolds at the injury site. In the hAECs transplanted group (group f), DII-labeled hAECs were gently injected into the lesion cavity with a Hamilton syringe. Then, the muscle and skin layers were sutured separately, and the mice were placed on the hot plate until they became conscious. After the surgery, enrofloxacin was injected subcutaneously in the arm of the animal at a dose of 5 mg/kg along with sterile distilled water for one week (Fig. 1a).

Assessment of locomotor behavior

The motor function of the right hind limb of the animal was evaluated through the motor scoring system Basso, Beattie, and Bresnahan (BBB) in an open field [24]. The BBB scale ranges from 0 (no hind limb movement) to 21 (natural movements, including coordinated walking with

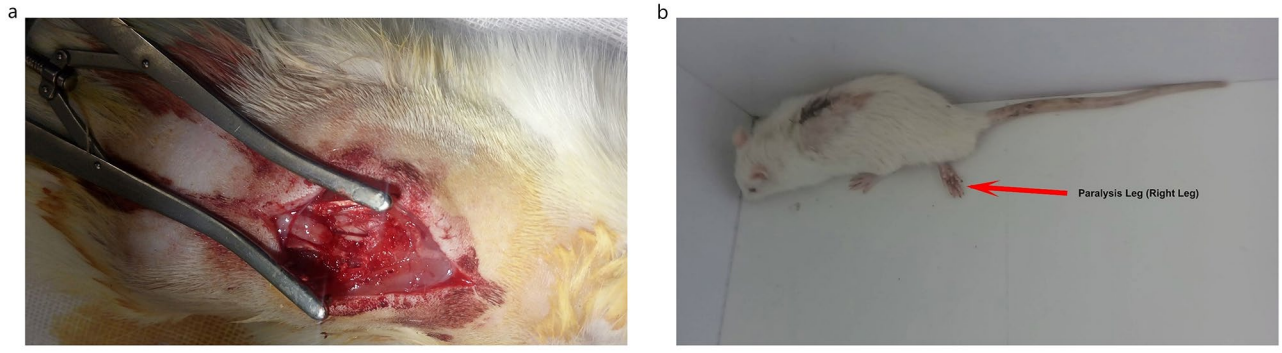

Fig. 1 **a**) A mouse undergoing surgery where the retractor has pushed aside the two muscle layers surrounding the vertebral column. **b**) The performance of the BBB Score test in the open field. The right leg is paralyzed after right hemisection surgery

paws parallel to the body). Rats were placed weekly in an open field for four weeks after surgery, and a 4-minute video was recorded. Besides, two blinded observers evaluated the hindlimb locomotor performance (Fig. 1b).

The expression level of neural markers for in vivo studies

The expression levels of the genes mentioned in the in vitro experiments section, including FOX3, GFAP, Calca, and MBP, were evaluated in spinal cord lesions of animal groups transplanted with hAECs using qPCR. In this way, the RNA of the spinal cord samples transplanted with the scaffold cultured with hAECs, transplanted with the scaffold loaded with Noggin along with hAECs, the group of hAECs alone, and the spinal cord lesion was extracted, and cDNA was synthesized accordingly. The following procedures were conducted as per the protocols of in vitro studies.

Histologic assessment

At the end of the study, euthanasia and tissue collection were carried out through intraperitoneal administration of 60 mg/kg ketamine combined with 10 mg/kg xylazine. Following this, transcardial perfusion was performed with 0.9% saline containing heparin to remove blood and minimize artifacts caused by blood components during fixation. The procedure was completed with perfusion of ice-cold 4% paraformaldehyde to preserve the tissues. After fixation, a part of the spinal cord, including the damaged and adjacent parts along with the vertebral bones, was cut off and embedded in a 4% paraformaldehyde solution for one week. Afterward, the spinal cord was carefully separated from the vertebrae and fixed again for five days in 4% paraformaldehyde. The selected samples were dehydrated with a tissue processor and molded with paraffin. Sections of 5 µm were prepared and used for H&E and immunofluorescent staining. H&E staining was used to show the location of the injury in the control group and the site of the scaffold in the injury cavity in the treatment groups. The stained samples were photographed using optical microscopes.

Immunohistochemistry (IHC) study

Initially, tissue samples were sectioned into slides with a thickness of 5 µm. Subsequently, the slides were subjected to a 90 °C oven for 15 min to facilitate the melting of the paraffin surrounding the samples, enabling deparaffinization. The sections were then immersed in Xylene to clarify and eliminate the paraffin from within the samples. Tissue sections were permeabilized with Triton 0.3%, and the secondary antibody reaction was blocked with 10% goat serum.

Diluted primary antibodies (1:1000), including GFAP, microglia, and macrophage-specific protein (Iba1), neuron-specific protein (β-tubulin), and myelin-specific protein (MBP), were added to the samples. Antibody-treated samples were placed in a refrigerator at 2 °C to 8 °C overnight. Samples were washed three times with PBS. The samples were incubated with a secondary antibody at 37 °C. After washing three times with PBS, DAPI was added to the samples. Finally, the samples were observed by a fluorescent microscope with standard fluorescent filters Labomed®TCS400 and ImageJ software was used to evaluate the immunohistochemical analyses.

Statistical analysis

Graph pad Prism 9 software program was used for the statistical analysis and drawing graphs. Data were presented as mean±SEM. ANOVA statistical analyzes were used to check the significance level of the difference in the experimental groups. A P -value less than 0.05 was considered significant. Statical significance was shown as follows *: $P<0.05$, **: $P<0.01$, ***: $P<0.001$, ****: $P<0.0001$.

Results

Isolation and culture of hAECs from human placentae

Human amniotic epithelial cells were harvested from amnion membranes of eligible healthy women after double-step enzymatic digestions. We evaluated the morphology and viability of isolated cells using by inverted microscope (Nikon ECLIPSE, TS100) and trypan blue, respectively. In this regard, over 95% of harvested cells were viable with elongation and spindle shape after three days (Fig. 2). Based on our previous immunocytochemistry evaluations of the pan-cytokeratin marker on isolated cells, over 98% of the cells tested positive for pan-cytokeratin [18].

Fabrication of the scaffold and attaching hAECs to the nanochitosan/PPy-Alg scaffold

In accordance with our previously established study protocol [21], the nanochitosan/PPy-Alg scaffold was fabricated. SEM images of hAECs cultured on the nanochitosan/PPy-Alg scaffold demonstrated successful attachment of hAECs to the scaffold surface after one week (Fig. 3). These findings indicated that hAECs adhered uniformly to the nanochitosan/PPy-Alg scaffold while maintaining their characteristic morphology.

Neural differentiation of hAECs on nanochitosan/PPy-Alg conductive scaffold in vitro

The expression of neuronal (Calca, Fox3), oligodendrocyte (MBP), and astrocyte (GFAP) genes extracted from hAECs cultured on nanochitosan/PPy–Alg scaffold was evaluated after 21 days. The result showed that the presence of Noggin, nanochitosan/PPy-Alg scaffold, or their combination increased the level of FOX3 neuronal gene expression in the hAECs. (Fig. 4A). However, both Calca

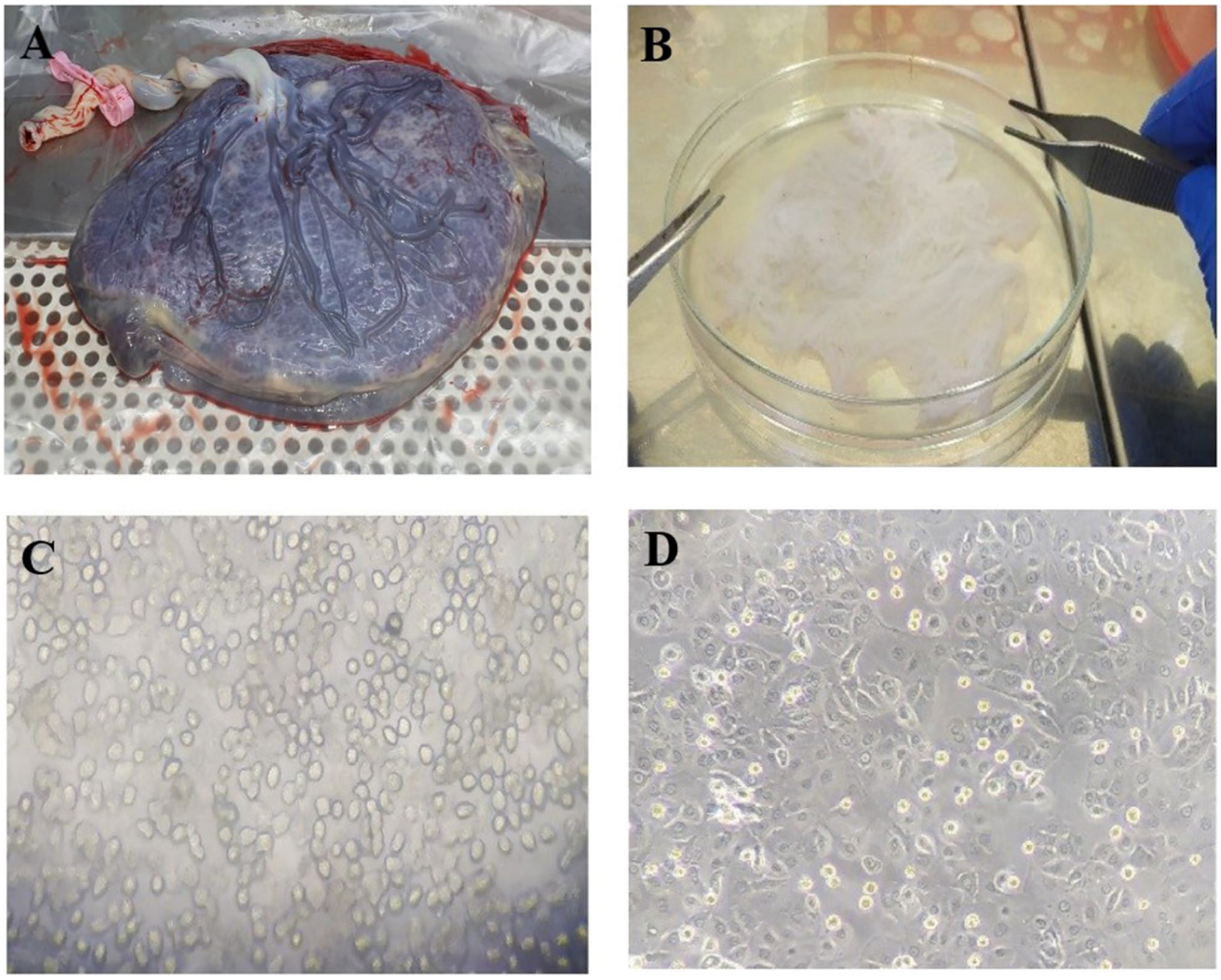

Fig. 2 The process of isolating hAECs from the amniotic membrane. **A**) The term human placenta was provided after elective Cesarean sections. **B**) Thoroughly washing the amniotic membrane with PBS. **C**) Evaluating the morphology of the cells on the day of isolation. **D**) Allowing the cells to reach 80% confluence three days after isolation

and MBP gene expressions showed significant increases in the cells cultured on the scaffold, regardless of the presence or absence of Noggin. (Fig. 4B, C).

After 21 days of culture, hAECs grown on the nanochitosan/PPy-Alg scaffold exhibited a significant increase in GFAP gene expression. In contrast, hAECs cultured without the scaffold did not show a significant increase in the expression of this gene, even in the presence of Noggin. (Fig. 4D). Additionally, in our previous study, we thoroughly evaluated the distribution and attachment of OLN-93 cells, a neural cell line, on the scaffold. Our results demonstrated that after 7 days, the cells were uniformly attached and evenly distributed throughout the scaffold [21].

Noggin protein loading on chitosan nanoparticles

Noggin, a known BMP signaling antagonist, is considered a neural differentiation growth factor. Since we aimed to investigate the therapeutic role of Noggin and nanochitosan/PPy–Alg conductive scaffold in SCI simultaneously, the interaction of nanochitosan particles as a scaffold component with active sites of Noggin was investigated using molecular simulation. The results showed that Hydrogen bonding of chitosan's OH and NH3 groups with Glu, Cys, Lys, Ser, and Trp amino acids caused the ligand binding and considerable stability in the Noggin active sites (Fig. 5).

After the bioinformatic study, the optical density (OD) of Noggin serial concentrations was assessed at 260 nm. The amount of Noggin loaded on chitosan nanoparticles was calculated based on formulas 1 and 2. The percent of loaded Noggin was 22.6%, and the entrapment efficiency was 75.3%.

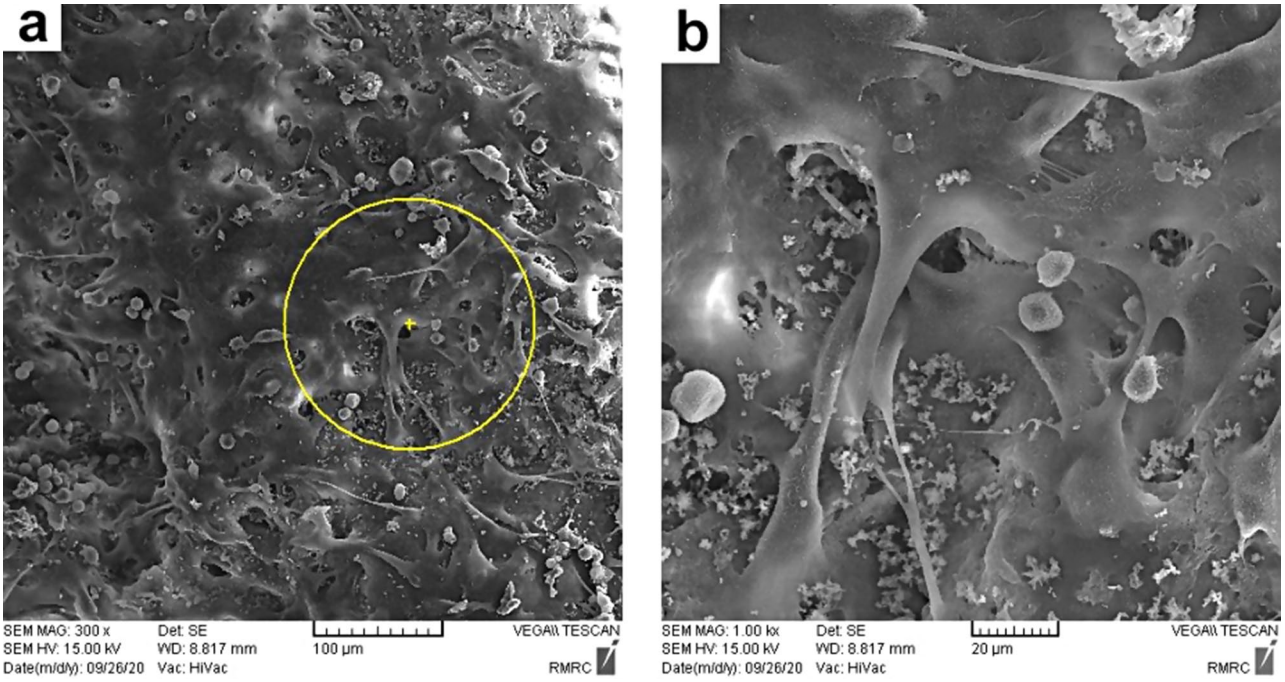

Fig. 3 **a**) Adhesion of hAECs cells on the Nanochitosan/PPy–Alg scaffold **b**) Magnified image of hAECs cells in the yellow circle area in Figure a

Release of Noggin from Noggin-loaded nanochitosan/PPy-Alg scaffold

The release of Noggin from the engineered scaffold was assessed for a duration of 12 days. The total amount of Noggin released during this period was determined to be 28.5%. Within the initial four days, 15% of Noggin was released, primarily attributed to the amount of Noggin that was initially attached to the surface of nanochitosan. Subsequently, the release process proceeded gradually over the following eight days, primarily influenced by the quantity of proteins incorporated within the chitosan nanoparticle matrix (Fig. 6).

Histology of the lesion site

The current study utilized the right hemisection spinal cord lesion model (Fig. 7). Following the immediate creation of the lesion in the experimental groups, the scaffold was transplanted into the T10-T11 region. To determine the positioning of the scaffold within the lesion site one week after transplantation, longitudinal sections of the control lesion and scaffold-treated samples were subjected to H&E staining. Macroscopic (Fig. 7A) and microscopic (Fig. 7C) observations of the lesion control group revealed an empty cavity devoid of cells at the center of the lesion (Fig. 7C). In contrast, the treatment group displayed a filled lesion cavity with the scaffold (Fig. 7B), forming a rostrocaudal connecting bridge across the lesion (Fig. 7D). Furthermore, the scaffold exhibited strong cohesion with the surrounding native tissue, and no scarring was observed in the transplanted group featuring an intermediate scaffold.

Motor behavior assessment (BBB)

To evaluate the therapeutic effect of nanochitosan/PPy–Alg conductive scaffold, animals grafted with nanochitosan/PPy–Alg scaffold (with and without hAECs and/or Noggin) were analyzed through BBB motor scoring once a week. All animals had normal motor functions before inducing SCI (BBB=21). The right lateral hemisection spinal cord lesion model was created that caused paralysis in the right hind limb in all experimental groups. Immediately after the injury, all groups showed similar BBB scores in which the right posterior limb muscle strength decreased from 21 to 0, causing ipsilateral paralysis of the hind limb. During the four-week evaluation period, the mice in all groups demonstrated gradual improvement in their BBB scores. However, a more peominent therapeutic effect was observed after transplanting nanochitosan/PPy-Alg scaffolds combined with hAECs and Nogging throughout the assessment duration. This indicates a substantial enhancement in motor function for the hind limbs, signifying a better improvement in the treated groups (Fig. 8). Significantly higher BBB scores were observed in the rats treated with the transplanted Noggin-loaded nanochitosan/PPy-Alg scaffold combined with hAECs (14 ± 1.43, $^{**}P<0.01$) compared to those in the scaffold alone, hAECs alone, and lesion groups after four weeks.

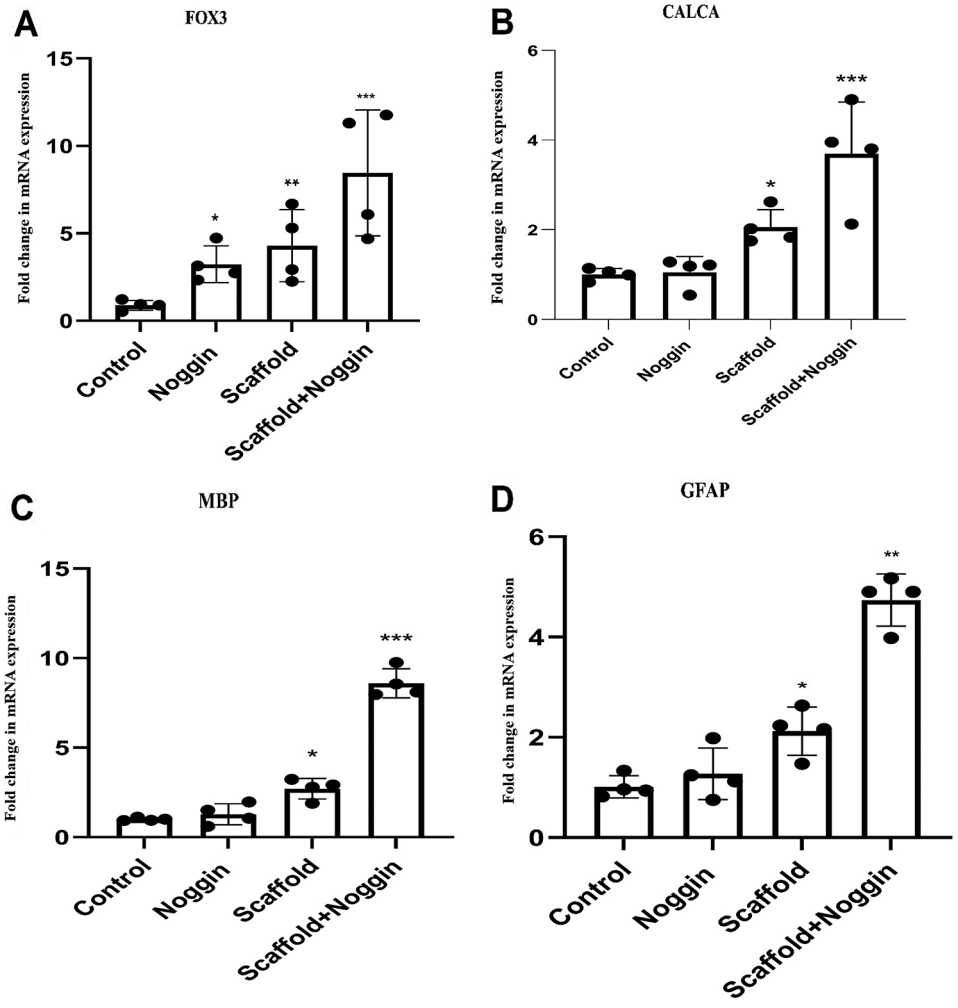

Fig. 4 Real-time PCR of neural marker genes expression in hAECs on nanochitosan/PPy–Alg scaffold in vitro after 21 days. (**A**) Real-time PCR of FOX3 gene expression, (**B**) CALCA gene expression in experimental groups, (**C**) MBP gene expression in experimental groups, and (**D**) GFAP gene expression in experimental groups (comparison was made with the control group, and data were presented as mean ± SEM). $^{*}P < 0.05$, $^{**}P < 0.01$, $^{***}P < 0.001$

Similarly, the group treated with the nanochitosan/PPy-Alg scaffold combined with hAECs showed improved BBB scores (13.5±0.7, $^{**}P<0.01$) vs. SCI group. Moreover, the rats treated with the Noggin-loaded nanochitosan/PPy-Alg scaffold alone also exhibited increased BBB scores (12.5±0.51, $^{*}P<0.05$) vs. SCI group. In contrast, the hAECs alone group achieved a BBB score of 10±1.41, while the control group had a BBB score of 9.5±1.52 that showed no significant difference (Fig. 8).

Exploring the in vivo neural differentiation of hAECs

The expression level of human neuronal (Calca, Fox3), oligodendrocyte (MBP), and astrocyte (GFAP) genes in animal samples extracted from SCI after four weeks were evaluated by RT-PCR. Considering RT-PCR findings, in untreated SCI mice, the human Calca, Fox3, MBP, and GFAP genes were not expressed. However, there was a notable increase in FOX3, CALCA, and MBP expression in the mice transplanted with Noggin-loaded scaffold along with hAECs compared to the control group (hAECs injected group). On the other hand, in both intervention groups, the astrocytic GFAP gene expression level was significantly lower, indicating a poor astrocytic phenotype in the improved SCI. (Fig. 9).

Immunofluorescence analysis of the inflammation responses

Inflammation impedes neural regeneration in the acute phase of SCI. In this study, anti-inflammatory effects and biocompatibility of nanochitosan/PPy–Alg scaffold, Noggin, hAECs, and their combination were assessed through assessing Iba1, a microglia/macrophage-specific calcium-binding protein, seven days after SCI induction (Supp Fig. 1). The IHC results showed that the Iba1 levels of two hAECs seeded scaffold transplanted groups (with and without Noggin) were significantly decreased (Fig. 10a).

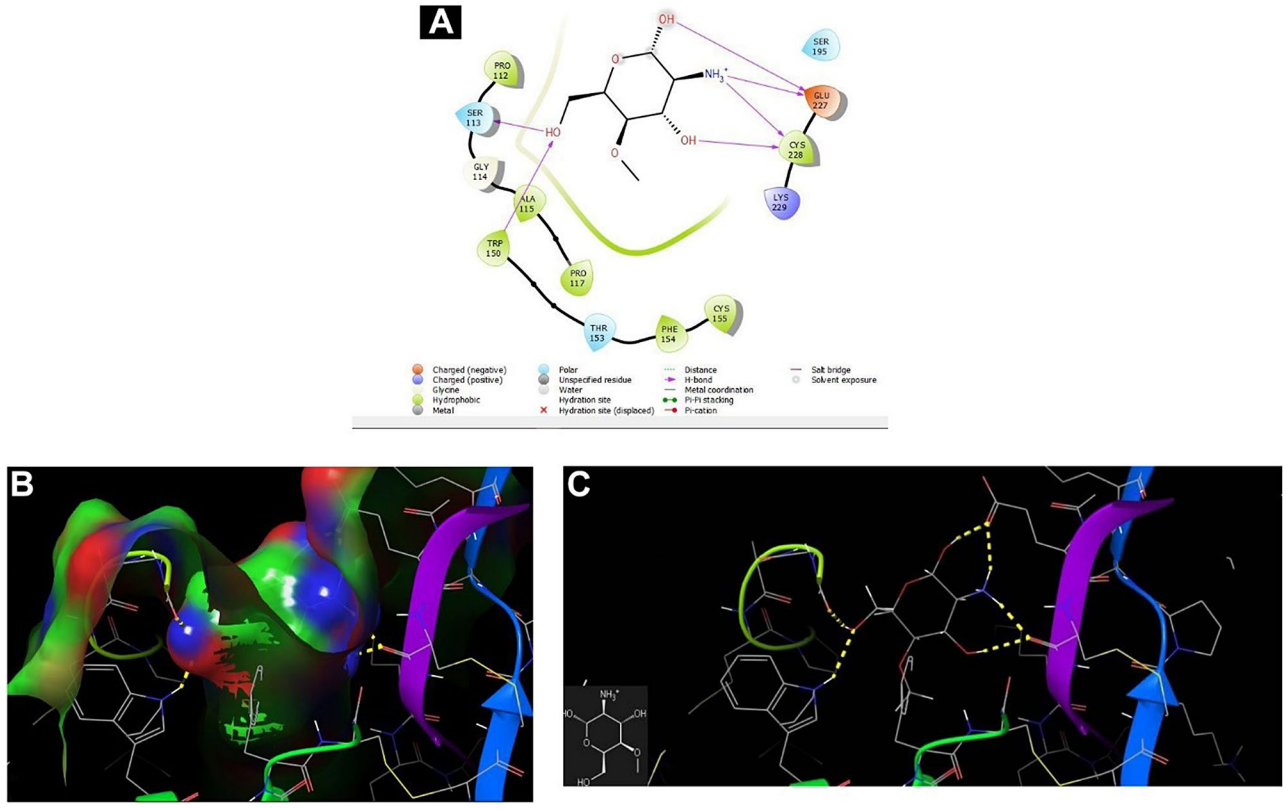

Fig. 5 **A**) the 2D structure of chitosan and Noggin interaction, where purple lines represent hydrogen bonds. **B** and **C**) 3D structure of chitosan and Noggin, where the interaction of hydrogen in OH and NH3 groups of chitosan with Glu, Cys, Lys, Ser, and Trp amino acids of Noggin resulted in chitosan-Noggin binding and stability

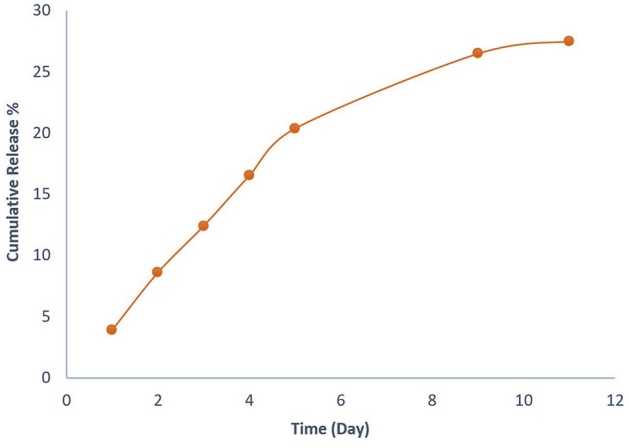

Fig. 6 The Noggin release profile from Noggin-loaded nanochitosan/PPy–Alg scaffold

Immunofluorescence analysis of the scar formation in SCI

Astrocytes constitute the primary component of the glial scar that forms after SCI, potentially impeding the recovery or regeneration process following the injury. This study analyzed the staining density of reactive astrocytes around the injury zone in grafted groups after four weeks. The results showed that GFAP$^+$ astrocytes were present around the injury area at the host/lesion boundary in all SCI groups (Supp Fig. 2). The density of GFAP staining around the injury site in scaffold groups and scaffold groups cultured with hAECs was significantly decreased compared to the lesion group ($^*P<0.05$). These findings indicate that the nanochitosan/PPy-Alg scaffold, Noggin, hAECs, and their combination transplantation significantly reduced the number of GFAP$^+$ astrocytes within the SCI lesions (Fig. 10b).

Immunofluorescence analysis of the nerve density in SCI

In order to evaluate the therapeutic effects of nanochitosan/PPy–Alg scaffold, Noggin, and hAECs on regeneration and sprouting of damaged nerve cells and axons in acute SCI, the density of nerve fibers was analyzed by immunofluorescence staining analysis of β-tubulin III (Supp Fig. 3) and MBP (Supp Fig. 4) at the lesion site. The results showed scaffold transplantation induced more nerve fibers in the lesion site four weeks after transplantation. Also, we observed a significant increase in nerve fibers density in the Noggin-loaded scaffold with the hAECs group compared to the nanochitosan/PPy–Alg scaffold group with hAECs that shows Noggin induced more prominent increase in β-tubulin+nerve fibers density (Fig. 10c). In addition, β-tubulin-positive nerve fibers have extended and grown toward the scaffold. The

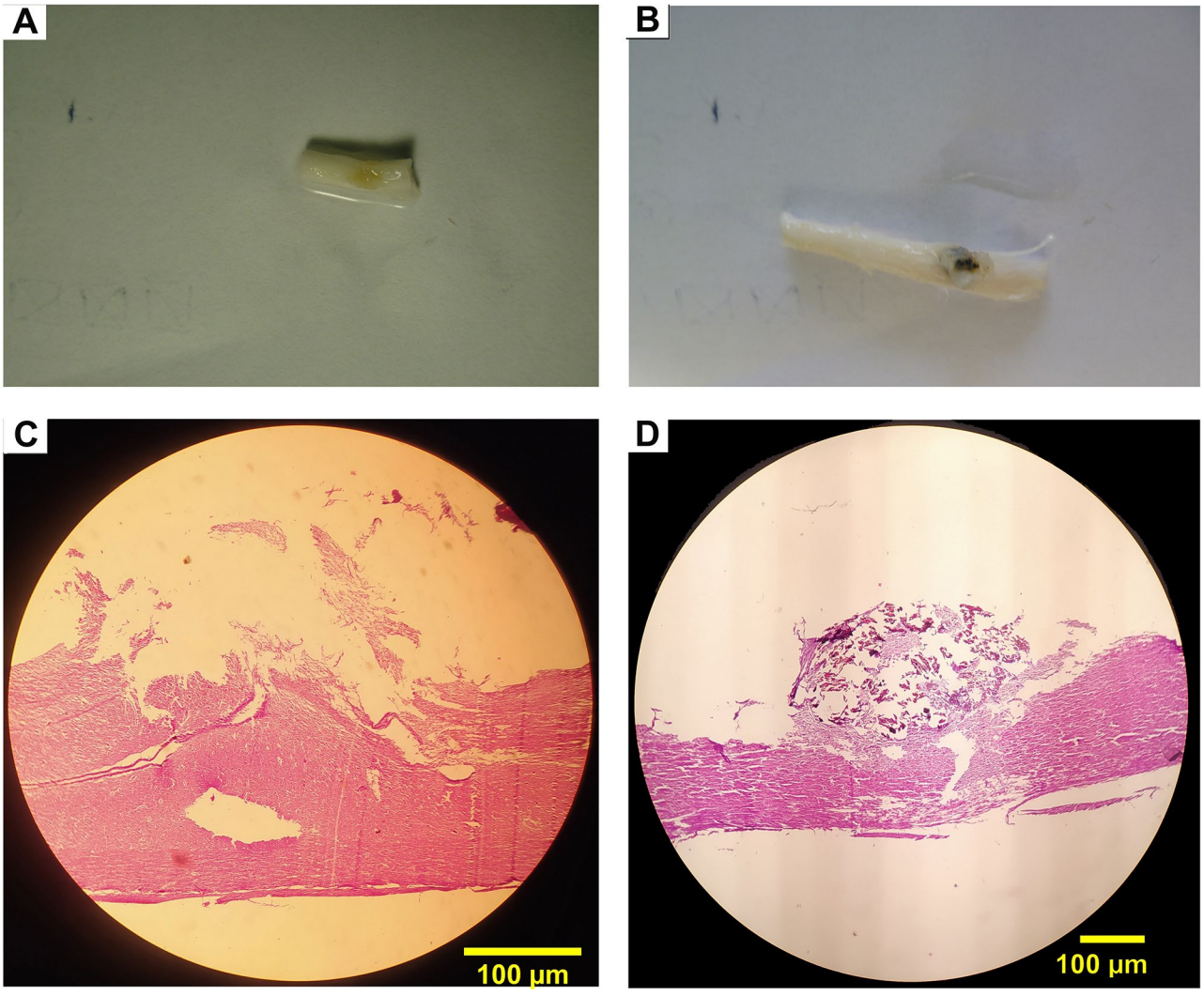

Fig. 7 Both the lesion group and the scaffold-treated lesion group were examined using macroscopic and microscopic images to assess the injured spinal cord. **A**) The macroscopic picture illustrates the injured spinal cord without any treatment, displaying the extent of the injury (Control). **B**) The macroscopic image depicts the injured spinal cord with the scaffold positioned at the injury site, demonstrating the application of the scaffold for treatment (Treatment). **C**) A microscopic image obtained from H&E staining reveals the gap formed at the injury site in the lesion group (Control). **D**) A microscopic image resulting from H&E staining displays the successful placement of the scaffold at the injury site in the lesion group that underwent scaffold transplantation (Treatment).

increase in cellular penetration in the scaffold-treated groups was associated with a significant increase in the density of nerve fibers determined by β-tubulin-stained fibers.

The remyelination of nerve fibers was observed by positive staining of MBP as a structural component of myelin exclusively expressed by mature oligodendrocytes. The evaluation showed that four weeks after the transplantation, more MBP-positive immunofluorescence fibers presented in all grafted groups except the Noggin-loaded scaffold without hAECs (Fig. 10d). Besides, the density of MBP nerve fibers was significantly increased in the Noggin-loaded scaffold with hAECs group compared to the nanochitosan/PPy–Alg scaffold group with hAECs which showed the possible effect of Noggin on the remyelination of nerve fibers.

Discussion

Neurodegenerative diseases such as SCI result from function loss of CNS cells in the brain or spinal cord. Along with the negligible ability of neurons to repair themselves during self-repairment, the survival and growth of these cells are reduced due to glial scar formation. Therefore, the reconstruction of the central nervous system has many challenges [25, 26]. Destruction of nerve cells, demyelination, and glial scar formation are destructive processes after SCI. Recently, several therapeutic

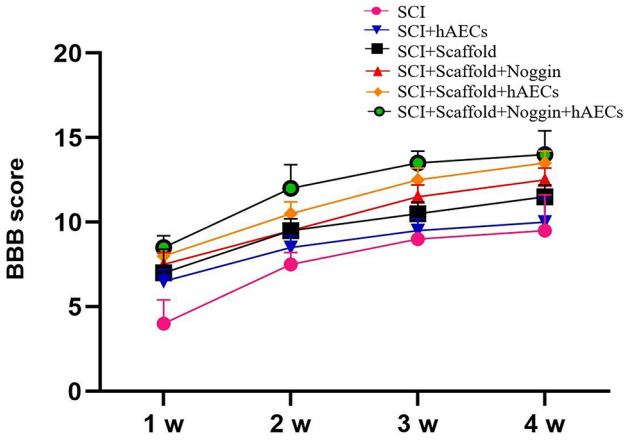

Fig. 8 The BBB movement scoring diagram was employed to assess the scores in various weeks following SCI. Throughout the four-week evaluation period, all groups of mice showed gradual improvement in their BBB scores. However, the groups that received the combination of hAECs, nanochitosan/PPy-Alg scaffolds and Noggin demonstrated a more pronounced therapeutic effect throughout the entire assessment duration

approaches based on the use of stem cells from various origins have been studied in the treatment of SCI.

The amniotic membrane is enriched with multipotent stem cells, including hAECs. It has been shown that hAECs are suitable for cell therapy in CNS injuries due to minor immune system rejection, low tumorigenicity, and differentiation capacity to nervous system cells. hAECs can express neuronal and neuroglia cell phenotypes such as MAP-2 and GFAP and neural stem cell markers such as nestin and musashi-1 [27, 28]. Thus, hAECs are potential candidates for regenerating the injured spinal cord. In this context, a study by WU Zhi-yuan et al. revealed that transplanted hAECs exhibited excellent survival in the injured neural tissue even after eight weeks. Notably, the transplantation process led to the filling of the lesion site without forming cysts or scars, which holds significant importance in promoting axonal regeneration in the CNS [28].

However, cell-based therapeutic methods yield minor functional improvements due to the lack of structural and biochemical frameworks for guiding, protecting, and stimulating the regrowth of axons in the damaged area. Scaffolds provide a suitable platform for cell transplantation to the lesion site or the simultaneous delivery of neurotrophic factors, as well as structural and chemical support for the regrowth of axons. However, there is a need to design scaffolds with appropriate mechanical properties and porosity to allow the regrowth of guided axons across the lesion [29]. In the current study, for the first time, we evaluated the neural differentiation of hAECs on a newly designed nanochitosan/PPy–Alg conductive scaffold. Besides, we developed a drug delivery system for Noggin in order to investigate the simultaneous effect of scaffold and Noggin, a nerve regeneration factor, on neuron regeneration inability and improving the motor function of the hemisection SCI animal model.

The non-toxicity of PPy–Alg composite has been studied in various studies [30, 31]. Besides, it has also been shown that combining chitosan with PPy–Alg composite provides a suitable substrate for interaction between cultured cells and the external electric field [31]. Huang et al. cultured various cells, including neurons, glial cells derived from dorsal root ganglia, endothelial cells, and mesenchymal cells on pyrrole-based scaffolds and evaluated the activity level, survival, morphology, and reproduction. They showed that pyrrole not only had no adverse effect on these cells but also increased their adhesion, proliferation, and activity [32]. In our study, the assessment of hAECs viability in the scaffold showed that nanochitosan/PPy–Alg scaffold did not reduce the viability of hAECs and is biocompatible. In addition, adhesion studies showed that hAECs were attached correctly and distributed in the nanochitosan/PPy–Alg scaffold.

Another critical step in regenerating functional nerves is reprogramming intracellular pathways to persuade hAECs to differentiate into nervous system cells. Some studies have revealed the pivotal role of BMP signaling in neural development [17]. Recently, we studied the impact of inhibiting BMP signaling using its antagonist, Noggin, on the neural differentiation of hAECs. The results demonstrated a notable increase in the expression of neuronal markers, specifically MAP2 and β-tubulin, indicating a significant enhancement in the process of neural differentiation [18]. As a novelty, our study demonstrated that hAECs cultured on nanochitosan/PPy–Alg scaffold, exposed to Noggin, expressed all three subtypes of nervous system cells, including neurons (FOX3, Calca), oligodendrocytes (MBP), and astrocytes (GFAP) during 21 days. In other words, this scaffold can differentiate cells into neural lineage due to its exclusive electrical and chemical properties.

In order to optimize the differentiation of the hAECs on the nanochitosan/PPy–Alg scaffold and develop effective nervous tissue in vivo, it is necessary to maintain sufficient amounts of differentiation factors, including Noggin, inside the scaffolds. Covalent binding to scaffold materials is one of the most commonly used methods for combining growth factors and scaffold molecules [33–35]. Since the study aimed to simultaneously investigate the potential effect of Noggin nerve growth factor and nanochitosan/PPy–Alg conductive scaffold in the healing of SCI, the interaction of nanochitosan particles as a scaffold component with the active site of Noggin protein was investigated using molecular simulation. Our bioinformatics evaluation indicated that the interactions of OH and NH3 groups of chitosan with Glu, Cys, Lys, Ser, and Trp amino acids of Noggin via hydrogen bondings caused proper stability in the Noggin active sites.

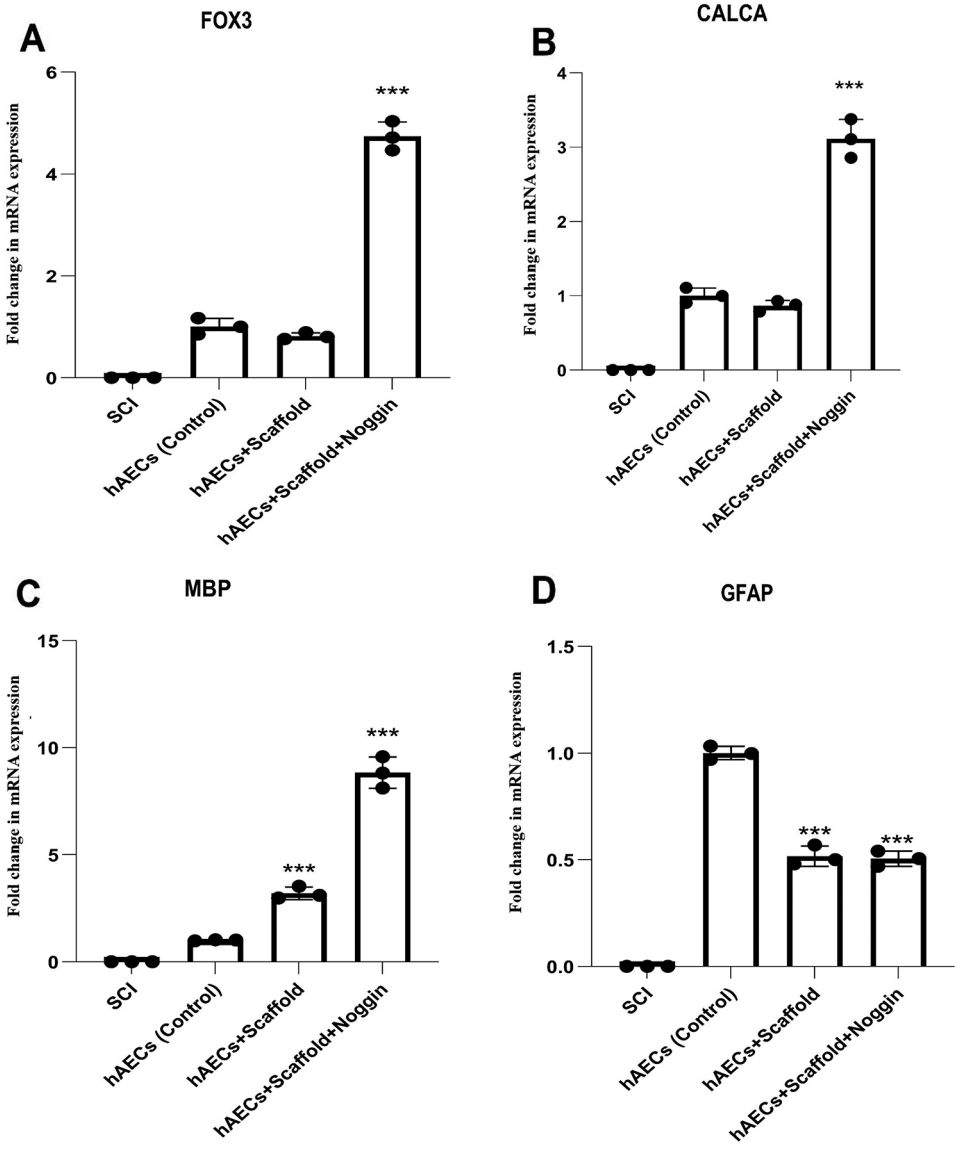

Fig. 9 Real-time PCR of neural marker genes expression after transplantation in vivo. (**A**) the expression level of FOX3 gene, (**B**) CALCA gene expression level, (**C**) MBP gene expression level, and (**D**) GFAP gene expression (comparison was made with the control group). ***$P < 0.001$ SCI: Spinal cord injury; AECs: Amniotic epithelial cells

Besides, Noggin was released slowly during 12 days from the scaffold, which was desirable considering the goal set for the slow release of Noggin over a long period in the body.

After transplantation of our regenerative system into the injured spinal cord, the macroscopic and microscopic results (H&E staining) showed that the scaffold was biocompatible with the host spinal cord tissue. The scaffold was adequately integrated with the spinal cord and filled the wound gap. Besides, neither scar tissues nor cystic cavities were observed. We noticed that our regenerative system improved the motor function of hemisected SCI animals in all tested weeks (1, 2, 3, 4) more than other SCI groups. This observation could be attributed to the potential protective effects of Noggin and hAECs on the preservation of remaining neurons at the lesion site, as well as the possible differentiation of hAECs into neurons and oligodendrocytes via Noggin differentiative effects.

In order to shed light on the underlying mechanisms of motor function improvement, we evaluated the alteration of cells and microenvironment patterns in the damage site. The gene expression pattern analysis revealed notable changes in the differentiation of hAECs when cultured on the nanochitosan/PPy–Alg scaffold supplemented with Noggin in vivo. Specifically, there was a significant increase in the differentiation of hAECs into neurons and oligodendrocytes at the lesion site. In contrast, the differentiation of these cells into astrocytes was

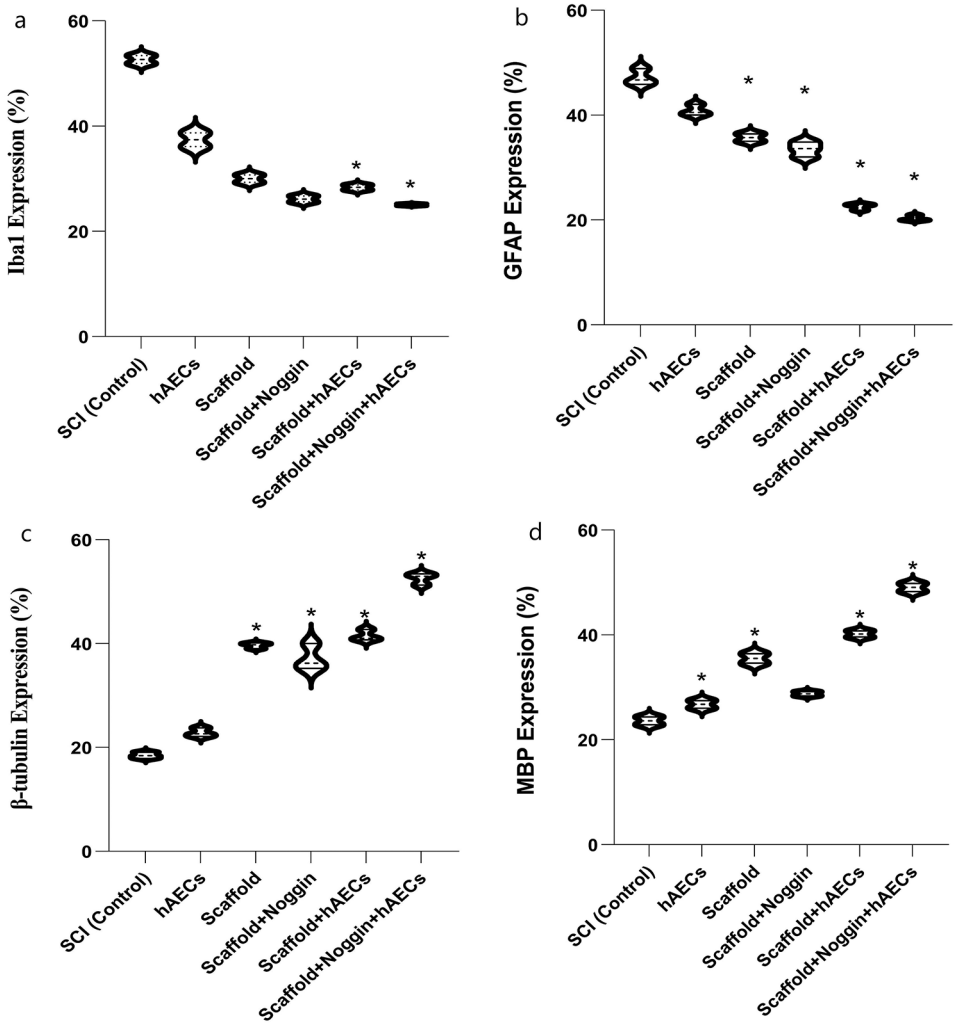

Fig. 10 Expression of specific neural and immune markers. Immunohistochemical analysis on longitudinal spinal cord sections in grafted spinal cords, stained for Iba1, GFAP, tubulin, MBP was evaluated by Image J software showed: **a**) significant decrease in Iba1 expression level within the SCI lesion, **b**) reduction in the number of GFAP$^+$ astrocytes within the SCI lesions, **c**) significant increase in the density of nerve fibers within the SCI lesions, **d**) significant increase in the density of nerve fibers within the SCI lesions. *$P < 0.05$ SCI: Spinal cord injury; AECs: Amniotic epithelial cells

reduced. This indicates that the presence of the PPy–Alg scaffold and Noggin played a role in limiting the differentiation of hAECs into astrocytes. The combination of the scaffold and Noggin appears to have directed the differentiation process towards neurons and oligodendrocytes instead, potentially contributing to the overall neural repair and regenerative outcomes observed in the study. Previous studies have shown that the expression of BMP4 increased in the acute phase of SCI, which limited neuronal and oligodendrocyte differentiation of transplanted cells and encouraged differentiation into astrocytes [36, 37].

Regulating immune reactions may be crucial as another possible therapeutic mechanism of our regenerative system. It has been suggested that leukocytes, especially T lymphocytes, and macrophages, infiltrating the injured spinal cord are directly involved in the pathogenesis and progression of SCI. In addition, some inflammatory processes, such as the production of cytokines, proteolytic enzymes, and oxidative metabolites, aggravate the injury [38]. Therefore, controlling inflammation promises to improve the recovery of SCI after the destruction of the spinal cord structure [39]. Considering that a damaged blood-brain barrier during the SCI process prone the spinal cord to leukocyte infiltration and inflammation, reconstructing or mimicking the function of the blood-brain barrier would enhance spinal cord regeneration [40]. In this regard, we showed that this regenerative system consisting of hAECs, Noggin, and nanochitosan/PPy–Alg scaffold reduced Iba1$^+$ cells (microglia and macrophages of peripheral origin) in the lesion site. The scaffold seemed to create a mechanical barrier that prevented immune cells and fibroblast infiltration into the lesion site. This mechanical blockage led to the reduction

of inflammatory responses and subsequently reduced the formation of scar tissue in the spinal cord. Besides, several studies have reported that hAECs possess the ability to modulate the immune system response by modifying the expression pattern of inflammatory cytokines through paracrine signaling or direct cell contact. hAECs release certain small molecules, such as IL-10 and prostaglandin E2 (PGE2), which play a crucial role in modulating inflammatory cells responsible for inflammation [41–43]. Additionally, hAECs can alter the polarization of macrophages, shifting them from the pro-inflammatory M1 phenotype to the anti-inflammatory M2 phenotype, which is associated with tissue repair and regeneration [44]. Moreover, hAECs express HLA-G, a non-classical HLA molecule, which helps regulate the immune response by promoting the expansion of regulatory T cells (Tregs) and inhibiting the activation of natural killer (NK) cells and dendritic cells [45]. This ability to modulate both innate and adaptive immune responses highlights the potential of hAECs to control inflammation and promote immune tolerance in pathological conditions characterized by immune dysregulation, such as in SCI. Considering the immunomodulatory roles of hAECs and Noggin, suppressing the inflammation may be attributed to the cooperation of the nanochitosan/ PPy–Alg scaffold, Noggin, and hAECs [10, 46].

Inhibitiong glial scar tissue formation as an additional potential therapeutic mechanism of our regenerative system induces successful tissue repair [47]. The combination of Nanochitosan/PPy–Alg scaffold, Noggin, and hAECs reduced the accumulation of $GFAP^+$ astrocytes at the border of the SCI lesion. Thus, astrocyte reduction increases the ability of axons to extend to the lesion site by diminishing inhibitory signals.

As the final evaluated mechanism, the primary objective in healing SCI is to promote the regeneration of damaged axons and guide them to reconnect with the pre-existing nerve cells at the lesion site. This process is critical for restoring neural connectivity and function in the injured spinal cord [48]. After four weeks, the combined action of Nanochitosan/PPy-Alg scaffold, Noggin, and hAECs resulted in enhanced proliferation of host cells and repair of axons at the injury site. Fibers were observed to grow towards the scaffolds. The viability of transplanted hAECs was assessed using DII staining, confirming that these cells could survive and exert their therapeutic effects for up to four weeks after transplantation. Furthermore, after transplantation, the scaffold showed the expression of neural (β-tubulin) and remyelination (MBP) markers, indicating the differentiation of the transplanted cells into neurons. Therefore, we showed that our drug delivery system supported neural tissue regeneration by increasing hAECs viability in the damaged area, providing a suitable bridge for guided axonal growth, corporating and sustain releasing of Noggin neural growth factor in the injured area, and modulating immune reaction resulting in lower scar formation and subsequently enhanced nerve fiber regeneration. A schematic summarizing the regenerative system components, preparation, and their proposed mechanisms of action is shown in Fig. 11.

There have been limitations in this study that need to be acknowledged. Animal models of SCI do not fully replicate the complex pathology of human SCI, particularly regarding the variability in injury severity and recovery potential [49]. In our study, potential variability may have arisen from factors such as differences in the precision of injury induction, individual biological responses among the rats, scaffold fixation in lesion site, variations in postoperative care. To minimize this variability, we standardized the injury induction process by employing a consistent hemisection protocol at the T10-T11 spinal level, performed by the same individual across all subjects. The day after surgery, the models with 0 BBB score for right lower extremity were included in the study to better represent SCI model [50, 51]. To efficiently fix the scaffold in the lesion site we used animal fascia which led to better outcome. These steps were taken to reduce inconsistencies and enhance the reliability of our data, but we acknowledge that inherent biological variability remains a limitation of the SCI model.

While this study provides promising evidence for the therapeutic effects of the nanochitosan/polypyrrole-alginate scaffold loaded with Noggin and hAECs, several factors warrant further investigation. For instance, longer-term animal studies are necessary to assess the durability and long-term efficacy of the treatment, especially in terms of functional recovery, tissue regeneration, and the prevention of long-term complications such as fibrosis or secondary injury. Additionally, larger sample sizes would help to strengthen the statistical power of the findings, reduce the potential for bias, and ensure that observed effects are consistently reproducible across a broader population. Finally, clinical translation should be considered, where the application of this therapeutic strategy in larger, more diverse cohorts and under varying conditions would further validate the results and provide insights into its potential application in human SCI treatments.

Conclusion

This study demonstrated the suitability of the nanochitosan/PPy-Alg scaffold for facilitating the attachment and differentiation of hAECs into various types of nervous system cells, including neurons, oligodendrocytes, and astrocytes. Animal investigations further revealed that the grafting of nanochitosan/PPy-Alg scaffold, along with Noggin-loaded nanochitosan/PPy-Alg scaffold and

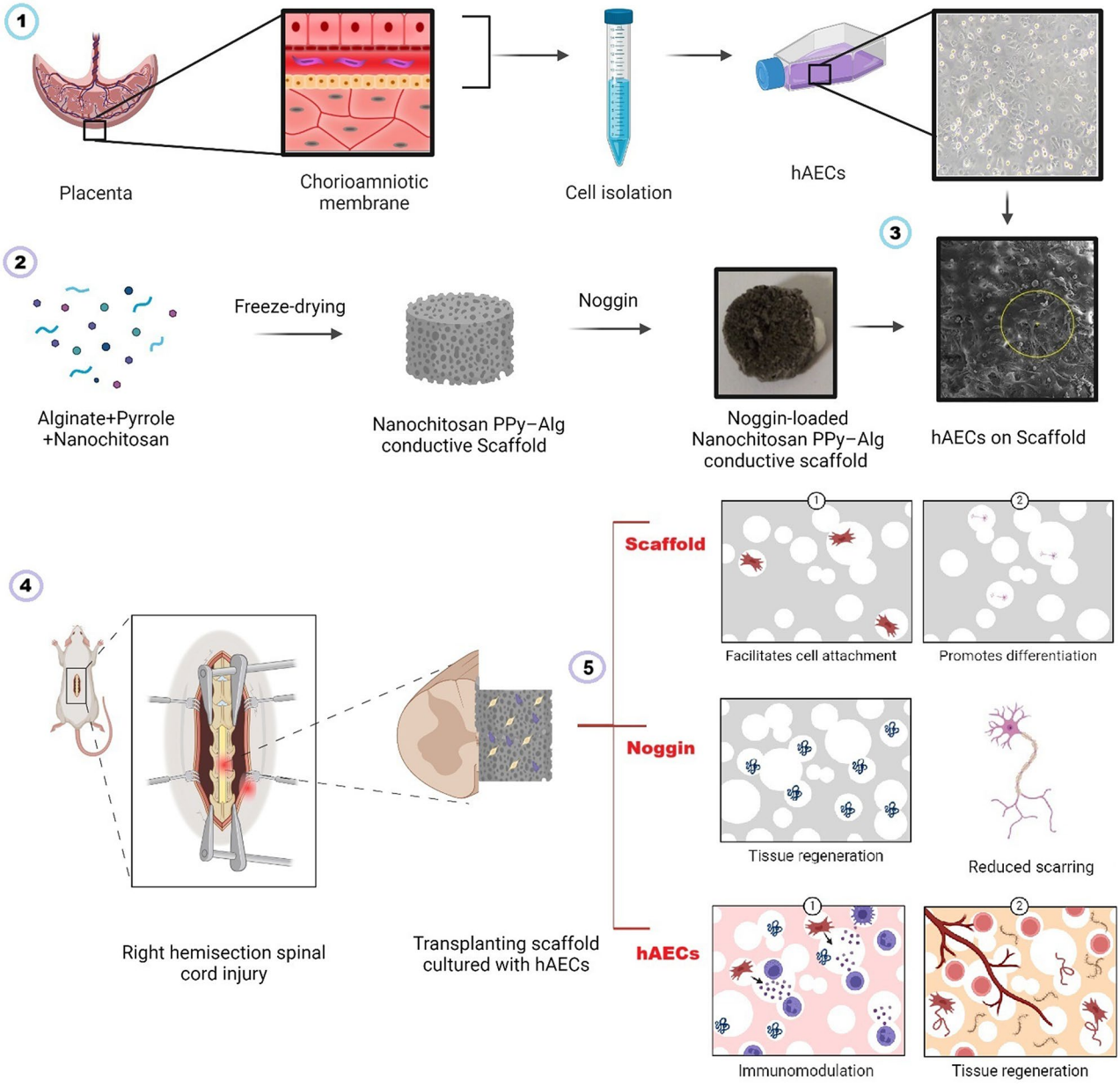

Fig. 11 The regenerative system for SCI treatment. (1) hAECs were isolated using an enzymatic digestion protocol. (2) The Nanochitosan/Polypyrrole-Alginate Conductive Scaffold was synthesized and loaded with Noggin. (3) The regenerative system, consisting of hAECs, the Nanochitosan/Polypyrrole-Alginate Scaffold, and Noggin, was prepared. (4) This system was grafted onto the SCI animal model. (5) Each component of the system played a crucial role in neural regeneration. The scaffold facilitated cell attachment, promoted differentiation, and provided mechanical support at the injury site. Noggin reduced scarring and enhanced neuroprotection and tissue regeneration by inhibiting BMP-mediated fibrosis. hAECs differentiated into neural cells, promoting tissue repair and regeneration. The system reduced inflammation and glial scarring, allowing better neural fiber regeneration. The combined effects led to improved motor function through enhanced neural network formation and functional recovery post-injury (designed by Biorender)

hAECs, exhibited several positive effects. These effects included the reduction of inflammation and glial scarring at the lesion site, promoting neural regeneration and remyelination. The hAECs cultured on the nanochitosan/PPy-Alg scaffold demonstrated long-term survival without provoking immune system rejection at the lesion site. Moreover, they induced axonal regeneration and sprouting, leading to improvements in motor functions of the hind limb through the release of neurotrophins. Overall, these findings suggest that the transplantation of Noggin-loaded PPy-Alg conductive scaffolds cultured with hAECs presents a novel approach in regenerative medicine and holds potential as a therapeutic strategy for SCI.

Supplementary Information

The online version contains supplementary material available at https://doi.org/10.1186/s13287-024-04104-5.

Supplementary Material 1

Acknowledgements
The authors would like to express their most sincere words of appreciation to personnel of Erfan Hospital for their valuable contribution. This work was supported by Vice-Chancellor in Research Affairs of Shahid Beheshti University of Medical Sciences, Tehran, Iran. Also, this research was supported by the Research Grant Committee from the National Institutes for Medical Research Development (NIMAD), Tehran, Iran, under award number of 963951.

Author contributions
AMT, HN, and A.M. contributed to the conception and study design. AMT carried out the experiments. NV contributed to the Real-Time PCR primer design. AMT, FS, and RT contributed to data or analysis tools and performed the analysis. SN contributed to the bioinformatics analysis. AB, AMT wrote the original draft. AB, AMT, SB, and HN contributed to the manuscript revision and editing. All the authors read and approved the submitted version.

Funding
The authors declare that this research did not receive any specific grant from public, commercial, or not-for-profit funding agencies.

Data availability
This article contains no supplementary information. The data that support the findings of this study are included in this article; further inquiries can be directed to the corresponding author.

Declarations

Ethics approval and consent to participate
All experimental procedures were done after approval of proposal entitled "The effect of BMP signaling inhibition in Human Amniotic Epithelial Stem cells Seeded on Conductive nanochitosan/polypyrrole-alginate Scaffold for Directional Growth of axon in Spinal cord-Injured Rats" by the ethics committee of Shahid Beheshti University of Medical Sciences (IR.SBMU.MSP.REC.1401.001) in 2022/04/12. Besides, the informed consent of the participation was obtained from individuals.

Consent for publication
The Authors grant the Publisher the sole and exclusive license of the full copyright in the Contribution, which licenses the Publisher hereby accepts. Consequently, the Publisher shall have the exclusive right throughout the world to publish and sell the Contribution in all languages.

Competing interests
The authors declare that the research was conducted in the absence of any commercial or financial relationships that could be construed as a potential conflict of interest.

Declarations of generative AI and AI-assisted technologies in the writing process
During the preparation of this work the authors used GPT-4 in order to improve readability and language. After using this tool, the authors reviewed and edited the content as needed and take full responsibility for the content of the publication.

Author details
[1]Department of Pharmacology, School of Medicine, Shahid Beheshti University of Medical Sciences, Tehran, Iran
[2]Department of Applied Cell Sciences, School of Advanced Technologies in Medicine, Tehran University of Medical Sciences, Tehran, Iran
[3]Rayan Research Center for Neurosciece and Behavior, Dept. of Biology, Faculty of Science, Ferdowsi University of Mashhad, Mashhad, Iran
[4]Department of Phytochemistry, Medicinal Plants and Drugs Research Institute, Shahid Beheshti University, Tehran, Iran
[5]Ludwig Boltzmann Institute for Experimental and Clinical Traumatology in AUVA Research Center, Vienna, Austria
[6] Department of Pharmacology and Toxicology, School of Pharmacy, Iran University of Medical Sciences, Tehran, Iran

Received: 23 January 2024 / Accepted: 8 December 2024
Published online: 23 December 2024

References

1. Shen H, Fan C, You Z, Xiao Z, Zhao Y, Dai J. Advances in Biomaterial-Based Spinal Cord Injury Repair. Adv Funct Mater. 2022;32(13):2110628.
2. Tong A-N, Zhang J-W, Zhou H-J, Tang H-H, Bai J-Z, Wang F-Y, Lv Z, Chen S-Z, Liu S-J, Liu J-S, et al. Ischemic damage may play an important role in spinal cord injury during dancing. Spinal Cord. 2020;58(12):1310–6.
3. Karsy M, Hawryluk G. Modern Medical Management of Spinal Cord Injury. Curr Neurol Neurosci Rep. 2019;19(9):65.
4. Tsintou M, Dalamagkas K, Seifalian AM. Advances in regenerative therapies for spinal cord injury: a biomaterials approach. Neural regeneration Res. 2015;10(5):726–42.
5. Ottosen CI, Steinmetz J, Larsen MH, Baekgaard JS, Rasmussen LS. Patient experience of spinal immobilisation after trauma. Scand J Trauma Resusc Emerg Med. 2019;27(1):1–6.
6. Badhiwala JH, Wilson JR, Witiw CD, Harrop JS, Vaccaro AR, Aarabi B, Grossman RG, Geisler FH, Fehlings MG. The influence of timing of surgical decompression for acute spinal cord injury: a pooled analysis of individual patient data. Lancet Neurol. 2021;20(2):117–26.
7. Liu Z, Yang Y, He L, Pang M, Luo C, Liu B, Rong L. High-dose methylprednisolone for acute traumatic spinal cord injury: a meta-analysis. Neurology. 2019;93(9):e841–50.
8. Case LC, Tessier-Lavigne M. Regeneration of the adult central nervous system. Curr Biol. 2005;15(18):R749–53.
9. Mahar M, Cavalli V. Intrinsic mechanisms of neuronal axon regeneration. Nat Rev Neurosci. 2018;19(6):323–37.
10. Babajani A, Moeinabadi-Bidgoli K, Niknejad F, Rismanchi H, Shafiee S, Shariatzadeh S, Jamshidi E, Farjoo MH, Niknejad H. Human placenta-derived amniotic epithelial cells as a new therapeutic hope for COVID-19-associated acute respiratory distress syndrome (ARDS) and systemic inflammation. Stem Cell Res Ther. 2022;13(1):126.
11. Niknejad H, Peirovi H, Jorjani M, Ahmadiani A, Ghanavi J, Seifalian AM. Properties of the amniotic membrane for potential use in tissue engineering. Eur Cell Mater. 2008;15:88–99.
12. Miki T. Stem cell characteristics and the therapeutic potential of amniotic epithelial cells. Am J Reprod Immunol. 2018;80(4):e13003.
13. Maymó JL, Riedel R, Pérez-Pérez A, Magatti M, Maskin B, Dueñas JL, Parolini O, Sánchez-Margalet V, Varone CL. Proliferation and survival of human amniotic epithelial cells during their hepatic differentiation. PLoS ONE. 2018;13(1):e0191489.
14. Wang G, Zhao F, Yang D, Wang J, Qiu L, Pang X. Human amniotic epithelial cells regulate osteoblast differentiation through the secretion of TGFβ1 and microRNA-34a-5p. Int J Mol Med. 2018;41(2):791–9.
15. Ilancheran S, Moodley Y, Manuelpillai U. Human fetal membranes: a source of stem cells for tissue regeneration and repair? Placenta. 2009;30(1):2–10.
16. Niknejad H, Deihim T, Ahmadiani A, Jorjani M, Peirovi H. Permanent expression of midbrain dopaminergic neurons traits in differentiated amniotic epithelial cells. Neurosci Lett. 2012;506(1):22–7.
17. Manzari-Tavakoli A, Babajani A, Farjoo MH, Hajinasrollah M, Bahrami S, Niknejad H. The Cross-Talks Among Bone Morphogenetic Protein (BMP) Signaling and Other Prominent Pathways Involved in Neural Differentiation. Front Mol Neurosci. 2022;15:827275.
18. Biniazan F, Manzari-Tavakoli A, Safaeinejad F, Moghimi A, Rajaei F, Niknejad H. The differentiation effect of bone morphogenetic protein (BMP) on human amniotic epithelial stem cells to express ectodermal lineage markers. Cell Tissue Res. 2021;383(2):751–63.
19. Shrestha S, Shrestha BK, Kim JI, Ko SW, Park CH, Kim CS. Electrodeless coating polypyrrole on chitosan grafted polyurethane with functionalized multiwall carbon nanotubes electrospun scaffold for nerve tissue engineering. Carbon. 2018;136:430–43.
20. Heidari M, Bahrami SH, Ranjbar-Mohammadi M, Milan P. Smart electrospun nanofibers containing PCL/gelatin/graphene oxide for application in nerve tissue engineering. Mater Sci engineering: C. 2019;103:109768.

21. Manzari-Tavakoli A, Tarasi R, Sedghi R, Moghimi A, Niknejad H. Fabrication of nanochitosan incorporated polypyrrole/alginate conducting scaffold for neural tissue engineering. Sci Rep. 2020;10(1):22012.
22. Biniazan F, Rajaei F, Darabi S, Babajani A, Mashayekhi M, Vousooghi N, Abdollahifar M-A, Salimi M, Niknejad H. Effects of Placenta-Derived Human Amniotic Epithelial Cells on the Wound Healing Process and TGF-β Induced Scar Formation in Murine Ischemic-Reperfusion Injury Model. Stem Cell Reviews Rep. 2022;18(6):2045–58.
23. Babajani A, Manzari-Tavakoli A, Jamshidi E, Tarasi R, Niknejad H. Anti-cancer effects of human placenta-derived amniotic epithelial stem cells loaded with paclitaxel on cancer cells. Sci Rep. 2022;12(1):18148.
24. Basso DM, Beattie MS, Bresnahan JC. A sensitive and reliable locomotor rating scale for open field testing in rats. J Neurotrauma. 1995;12(1):1–21.
25. Rajabian A, Rameshrad M, Hosseinzadeh H. Therapeutic potential of Panax ginseng and its constituents, ginsenosides and gintonin, in neurological and neurodegenerative disorders: a patent review. Expert Opin Ther Pat. 2019;29(1):55–72.
26. Pchitskaya E, Popugaeva E, Bezprozvanny I. Calcium signaling and molecular mechanisms underlying neurodegenerative diseases. Cell Calcium. 2018;70:87–94.
27. Wang TG, Xu J, Zhu AH, Lu H, Miao ZN, Zhao P, Hui GZ, Wu WJ. Human amniotic epithelial cells combined with silk fibroin scaffold in the repair of spinal cord injury. Neural Regen Res. 2016;11(10):1670–7.
28. Wu ZY, Hui GZ, Lu Y, Wu X, Guo LH. Transplantation of human amniotic epithelial cells improves hindlimb function in rats with spinal cord injury. Chin Med J (Engl). 2006;119(24):2101–7.
29. Kubinová Š, Horák D, Hejčl A, Plichta Z, Kotek J, Proks V, Forostyak S, Syková E. SIKVAV-modified highly superporous PHEMA scaffolds with oriented pores for spinal cord injury repair. J Tissue Eng Regen Med. 2015;9(11):1298–309.
30. Ketabat F, Karkhaneh A, Mehdinavaz Aghdam R, Hossein Ahmadi Tafti S. Injectable conductive collagen/alginate/polypyrrole hydrogels as a biocompatible system for biomedical applications. J Biomater Sci Polym Ed. 2017;28(8):794–805.
31. Sajesh KM, Jayakumar R, Nair SV, Chennazhi KP. Biocompatible conducting chitosan/polypyrrole-alginate composite scaffold for bone tissue engineering. Int J Biol Macromol. 2013;62:465–71.
32. Huang Z-B, Yin G-F, Liao X-M, Gu J-W. Conducting polypyrrole in tissue engineering applications. Front Mater Sci. 2014;8(1):39–45.
33. Ho JE, Chung EH, Wall S, Schaffer DV, Healy KE. Immobilized sonic hedgehog N-terminal signaling domain enhances differentiation of bone marrow-derived mesenchymal stem cells. J Biomed Mater Res A. 2007;83(4):1200–8.
34. Gomez N, Schmidt CE. Nerve growth factor-immobilized polypyrrole: bioactive electrically conducting polymer for enhanced neurite extension. J Biomed Mater Res A. 2007;81(1):135–49.
35. Willerth SM, Rader A, Sakiyama-Elbert SE. The effect of controlled growth factor delivery on embryonic stem cell differentiation inside fibrin scaffolds. Stem Cell Res. 2008;1(3):205–18.
36. Setoguchi T, Nakashima K, Takizawa T, Yanagisawa M, Ochiai W, Okabe M, Yone K, Komiya S, Taga T. Treatment of spinal cord injury by transplantation of fetal neural precursor cells engineered to express BMP inhibitor. Exp Neurol. 2004;189(1):33–44.
37. Enzmann GU, Benton RL, Woock JP, Howard RM, Tsoulfas P, Whittemore SR. Consequences of noggin expression by neural stem, glial, and neuronal precursor cells engrafted into the injured spinal cord. Exp Neurol. 2005;195(2):293–304.
38. Wang YH, Chen J, Zhou J, Nong F, Lv JH, Liu J. Reduced inflammatory cell recruitment and tissue damage in spinal cord injury by acellular spinal cord scaffold seeded with mesenchymal stem cells. Exp Ther Med. 2017;13(1):203–7.
39. Li X, Xiao Z, Han J, Chen L, Xiao H, Ma F, Hou X, Li X, Sun J, Ding W, et al. Promotion of neuronal differentiation of neural progenitor cells by using EGFR antibody functionalized collagen scaffolds for spinal cord injury repair. Biomaterials. 2013;34(21):5107–16.
40. Kushchayev SV, Giers MB, Hom Eng D, Martirosyan NL, Eschbacher JM, Mortazavi MM, Theodore N, Panitch A, Preul MC. Hyaluronic acid scaffold has a neuroprotective effect in hemisection spinal cord injury. J Neurosurg Spine. 2016;25(1):114–24.
41. Lebreton F, Hanna R, Wassmer CH, Bellofatto K, Perez L, Othenin-Girard V, de Tejada BM, Cohen M, Berishvili E. Mechanisms of Immunomodulation and Cytoprotection Conferred to Pancreatic Islet by Human Amniotic Epithelial Cells. Stem Cell Rev Rep. 2022;18(1):346–59.
42. Griffiths C, Charlton C, Scott W, Ali S, Fisher AJ. Evaluating the immunomodulatory potential of human amniotic epithelial cells as a therapeutic in ex vivo donor lung reconditioning. Cytotherapy. 2019;21(5):S49–50.
43. Zhang Q, Lai D. Application of human amniotic epithelial cells in regenerative medicine: a systematic review. Stem Cell Res Ther. 2020;11(1):439.
44. Magatti M, Vertua E, De Munari S, Caro M, Caruso M, Silini A, Delgado M, Parolini O. Human amnion favours tissue repair by inducing the M1-to-M2 switch and enhancing M2 macrophage features. J Tissue Eng Regen Med. 2017;11(10):2895–911.
45. Morandi F, Marimpietri D, Görgens A, Gallo A, Srinivasan RC, El-Andaloussi S, Gramignoli R. Human Amnion Epithelial Cells Impair T Cell Proliferation: The Role of HLA-G and HLA-E Molecules. Cells 2020, 9(9).
46. Xiao Q, Du Y, Wu W, Yip HK. Bone morphogenetic proteins mediate cellular response and, together with Noggin, regulate astrocyte differentiation after spinal cord injury. Exp Neurol. 2010;221(2):353–66.
47. Nazemi Z, Nourbakhsh MS, Kiani S, Heydari Y, Ashtiani MK, Daemi H, Baharvand H. Co-delivery of minocycline and paclitaxel from injectable hydrogel for treatment of spinal cord injury. J Controlled Release. 2020;321:145–58.
48. Liu J, Chen J, Liu B, Yang C, Xie D, Zheng X, Xu S, Chen T, Wang L, Zhang Z, et al. Acellular spinal cord scaffold seeded with mesenchymal stem cells promotes long-distance axon regeneration and functional recovery in spinal cord injured rats. J Neurol Sci. 2013;325(1–2):127–36.
49. Alizadeh A, Dyck SM, Karimi-Abdolrezaee S. Traumatic Spinal Cord Injury: An Overview of Pathophysiology, Models and Acute Injury Mechanisms. Front Neurol. 2019;10:282.
50. Song RB, Basso DM, da Costa RC, Fisher LC, Mo X, Moore SA. Adaptation of the Basso-Beattie-Bresnahan locomotor rating scale for use in a clinical model of spinal cord injury in dogs. J Neurosci Methods. 2016;268:117–24.
51. Lebedev SV, Timofeyev SV, Zharkov AV, Schipilov VG, Chelyshev JA, Masgutova GA, Chekhonin VP. Exercise Tests and BBB Method for Evaluation of Motor Disorders in Rats after Contusion Spinal Injury. Bull Exp Biol Med. 2008;146(4):489–94.

Publisher's note